Journal of Agrometeorology

ISSN : 0972-1665 (print), 2583-2980 (online)
Vol. No. 26 (4) : 411-418 (December - 2024)
https://doi.org/10.54386/jam.v26i4.2756
https://journal.agrimetassociation.org/index.php/jam

Research Paper

Assessment of air pollution dispersion during wet season: A case study of Rumaila Combined Cycle Power Plant, Basrah, Iraq

MARIAM S. NASSER[1*], JINAN S. AL-HASSANY[1] and MONIM H. AL-JIBOORI[2]

[1]*Department of Biology, College of Science for Women, University of Baghdad, Iraq, Baghdad, Iraq.*
[2]*Department of Atmospheric Science, College of Science, Mustansiriyah University, Baghdad, Iraq.*
[*]*Corresponding author E-mail:* mariam.salah2202m@csw.uobaghdad.edu.iq

ABSTRACT

This study presents an assessment of the levels of air pollution emanating from natural gas combustion at the Rumaila Combined Cycle Power Plant (CCPP) in Basrah City by using a Gaussian dispersion model, with results at distance of 100, 500 and 1000 m for the pollutants CO, SO_2, NO, and particulate matters (PM). Data on atmospheric stability assessments were taken from meteorological stations in Basrah Governorate that belong to the Iraqi Ministry of Agriculture. The study determined the emission rates from the five stacks of the plant and the wind speed, wind direction at stack height, and Turner-Pasquill stability classes for the wet conditions of 2023/2024. The following are the maximum pollutant concentrations emanating from the stacks: CO was 186 $\mu g.m^{-3}$ at 100 m, 6 $\mu g.m^{-3}$ at 500 m, and 2.5 $\mu g.m^{-3}$ at 1000 m; SO_2 was 0.5 $\mu g.m^{-3}$ at 100 m, 0.05 $\mu g.m^{-3}$ at 500 m, and 0.01 $\mu g.m^{-3}$ at 1000 m; NO was 0.07 $\mu g.m^{-3}$ at 500 m and 0.03 $\mu g.m^{-3}$ at 1000 m; PM was 11 $\mu g.m^{-3}$ at 100 m, 0.4 $\mu g.m^{-3}$ at 500 m, and 0.15 $\mu g.m^{-3}$ at 1000 m. All of these measurements are well below national ambient air quality standards, which means that the Rumaila power plant is not locally deleterious to the air quality.

Keywords: Pollutants, Emission rate, Atmospheric stability, Gaussian model. Standard weather station, Pollutant dispersion

Air pollution results from noxious substances in the air that have adverse effects on human health and the environment. Criterial pollutants consist of ozone (O_3), nitrogen dioxide (NO_2), sulfur dioxide (SO_2), carbon monoxide (CO), $PM_{2.5}$, and PM_{10}, which linger without natural attenuation and are able to cause many health risks (Abdel-Razzaq *et al.,* 2023). The intrinsic connection between the atmosphere and pollution impacts the composition of the atmosphere, climate, and environmental quality. The Surface Boundary Layer (SBL), which is situated few meters above the land surface, is very important for the exchange of energy, dispersion of pollutants, and meteorological processes. Being 10% of the Atmospheric Boundary Layer (ABL), SBL undergoes turbulence and vertical mixing that make it impulsive to a large variety of weather systems and distribution of pollutants curtailing climate dynamics and ecosystem stability (Khadir *et al.,* 2024; Anand and Pal, 2023; Wu *et al.,* 2021).

Speaking technically, natural gas is mostly methane and considered by 20th-century analysts as a clean energy source that dampens climate change and promotes sustainable development by reducing PM (Wang *et al.,* 2024). Combustion of natural gas results in much lower levels of CO_2, NOx, and SO_2 compared to coal; CO emissions range from 0.1-0.5 $g.kWh^{-1}$ compared to 1.0-3.0 $g.kWh^{-1}$ for coal (Karmaker *et al.,* 2020). Natural gas combustion typically results in 50-60% less NOx than coal and drastically fewer particulates.

In their paper dated (Vandani *et al*., 2016) made it clear that efficiencies of approximately 60% separate Combined Cycle Power Plants (CCPPs) from the much less efficient single-cycle plants. Typically, emissions from natural gas combined heat and power plants come under the National Ambient Air Quality Standards information provided by Ghosh *et al.,* (2023). Particularly in the Rumaila area of Basrah, Iraq, air quality is badly compromised due to raised levels of $PM_{2.5}$ and PM_{10}, which has significant health implications for respiratory and cardiovascular diseases among others, aggravated by the industrial activities (Talib and Zainab, 2021). Both formation and distribution of fine particulate

Article info - DOI: *https://doi.org/10.54386/jam.v26i4.2756*
Received: 27 September 2024; Accepted: 25 October 2024; Published online : 01 December 2024

matter are strongly dependent on humidity, chemical reactions are enhanced that produce HNO_3 and H_2SO_4 both key components in the formation of fine particles. Water droplets can act as coagulation centers for pollutants, leading to an increase in particle size and time spent in the atmosphere. High humidity also reduces wind speeds, which could otherwise disperse the pollutants (Wang *et al.,* 2022). These findings underscore the need for the challenges of air quality to be addressed by interdisciplinary methods (Jasim *et al.,* 2018). The research will study the wet period, from October 2023 to May 2024, as described by (Al-Muhyi and Aleedani, 2022) and assess how in a moist climate variation in solar radiation affect dispersion of pollutants, and, through this Earth's energy balance, temperature gradients, and wind patterns. In most cases, along with low wind, high humidity is a major factor in the dispersion of pollution. NOx and SO_2 are turned into acids, which are more harmful to aquatic ecosystems and vegetation. High humidity increases the rate at which the surrounding infrastructure of a power plant corrodes. This leads to increased chances of leaks for pollutants. The Rumaila combined cycle power plant (RCCPP) is one of the major actions for sustainable energy.

This research paper will assess the emissions of CO, SO_2, NO, and PM from the RCCPP and use a simplified Gaussian dispersion model to calculate pollutant concentrations at distances of 100, 500, and 1000 meters under different meteorological conditions. This can then be compared to assess its environmental impact and local air quality over the area. Such data are of prime importance in the definition of regions where permissible concentration standards may be exceeded.

MATERIALS AND METHODS

Study area

Rumaila combined cycle power plant (RCCPP), commissioned by the Iraqi Ministry of Electricity in 2015 and expanded in 2018 with the addition of two steam units, is a state-of-the-art power generation facility. Developed and operated by Kar Investment Company at north Rumaila within Al-Zubair District, Basrah Governorate, Iraq, which is about 50 km west of Basrah city center (30.5444375° N, 47.4049375° E) spanning 1,000 m by 900 m in the desert region rich in oil resources.

The RCCPP integrates both simple and combined cycle technologies for effective power generation. There are five simple cycle operated gas turbines and two combined cycle units for optimal energy recovery had made up this configuration. In the combined cycle configuration, heat recovery steam generators are used for the recovering of waste heat which is thrown off from gas turbines. The steam generators use the heat to convert water from the river, which in this case is a branch from Karma Ali River, which known as Abu Abdullah canal located to the north of Shatt al-Arab (30.5699198° N, 47.6985041° E). The produced steam will be used to run other turbines which will increase the over plant output. Liquid discharge from the power plant is into Shatt al-Basrah Canal (30.5187625° N, 47.7224844° E). A total installed capacity of 3,180 MW was engineered for the RCCPP to be maximized for energy efficiency with minimum possible impact on the environment, as shown in Fig. 1 Power Plant location in Basrah Governorate.

Automatic weather station

The Model 110-WS-25 meteorological instrument is designed for real-time atmospheric monitoring and data acquisition. It is equipped with a standard suite of sensors to measure six critical meteorological parameters: wind speed, wind direction, air temperature, relative humidity, barometric pressure and precipitation. In addition, the system allows for the integration of additional sensors to expand its measurement capabilities. The station, managed by the Iraqi Ministry of Agriculture, is located in Burjesia, Al-Zubair district, with geographic coordinates of 30.28° N latitude and 47.05° E longitude. It is located approximately 26 km from the RCCPP, as shown in Fig. 2a. The study covered the wet season, which are eight months starting from October 2023 and ending in May 2024,

Gaseous monitoring device

The PS7400 Gaseous Analyzer, manufactured in China, provides detailed analysis of flue gas components and is widely utilized for continuous monitoring in industries such as metallurgy, chemicals, building materials, waste treatment, incineration, and thermal power generation. At the RCCPP, this system is employed to monitor emissions resulting from the continuous operation and substantial natural gas consumption powering five simple cycle gas turbines. The plant releases flue gases through five stacks, each equipped with pollution sensors. The PS7400 system measures concentrations of (CO, SO_2, NO, PM), as well as operational parameters including temperature, pressure, humidity, and gas flow, as illustrated in Fig. 2b. The system includes analytical instrumentation, gas sampling equipment, a sample gas line, sample gas condensation equipment, and a condensate drainage system.

Dispersion Gaussian model

Gaussian model is one of the earliest models in solving air pollution problems is the as the pollutants under consideration are close to normal in their propagation. The Gaussian atmospheric dispersion model is based on the essential aspect of predicting pollutant concentration and distribution levels at receptor locations downwind emanating from point sources. It works with the prime assumption of being able to forecast pollutant dispersion based on the prevailing meteorological conditions and describes uniformly turbulent behaviour for the dispersion of pollutants which are being released into flow. Accurate predictions require as inputs accurate emission rates, wind speed at the source, and atmospheric stability; diurnal and seasonal variation of each of those parameters is known for an accurate prediction needed as input. In the study, surface-level pollutant concentrations were estimated using a modified Gaussian equation. Equation is based on the stipulation that modifications to the conventional Gaussian model were made for accurate prediction of ground-level concentration and evaluation of impact on human health and vegetation. To apply the Gaussian dispersion equation, the following parameters are required:

Emission rate

Emission rate is a description of how much of a pollutant is released per unit time and is key to predicting pollutant

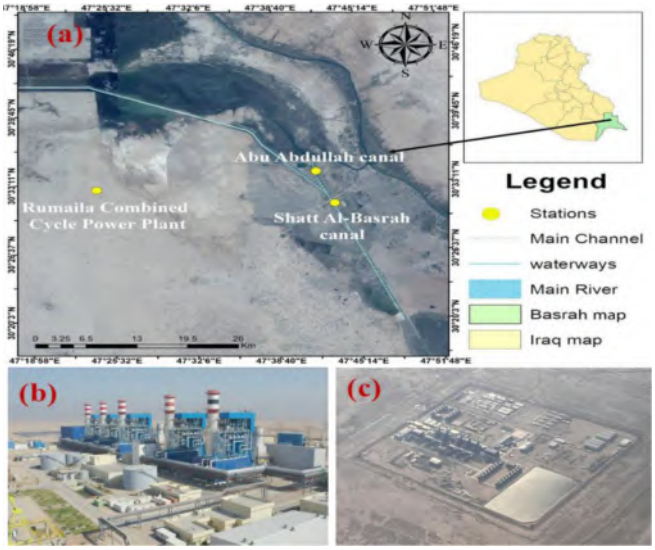

Fig. 1: Location of RCCPP, (a) Basrah city within RCCP lactation, (b) RCCPP photo with its five stacks, (c) RCCPP location from satellite.

concentrations at receptor downwind locations. Usually expressed in units such as tonnes per year, grams per second or kilograms per hour, this parameter is of fundamental importance to air quality modelling via its indication of source strength and influence on dispersion prediction in Gaussian plume models. At the RCCPP, stack gas exit velocities were measured for five stacks (60 meters high, 7.5 meters diameter) during the wet conditions. These velocities were then used in Eq. 1, which represent the volumetric flow rate of the stack (Beychok, 1994):

$$E_s\left(\frac{m^3}{sec}\right) = Vs * \frac{\pi * D^2}{4} \quad (1)$$

Where (Es) is Volumetric gas flow rate within the stack ($m^3.s^{-1}$), (D) is Diameter of the stack (m), (Vs) is Exit velocity from the stack ($m.s^{-1}$).

Adjustment to the flue gas flow rate must be made for moisture content and standard atmospheric conditions. It is done by the equation:

$$E_{s.dry}\left(\frac{m^3}{sec}\right) = E_s * \frac{273.15}{T_{actual}} * \frac{P_{actual}}{1_{atm}} (1 - fraction\ water\ vapour) \quad (2)$$

Where (P actual) is the actual internal pressure (in the stack) measured in ATM, (T actual) is the actual internal temperature (in the stack) measured in Kelvin. The emission rate in grams per second ($g.s^{-1}$) for certain gas in $g.m^{-3}$ at the stack was given as by the following equation (Beychok, 1994):

$$Q_s = E_{s.dry}\left(\frac{m^3}{s}\right) C_0 \left(\frac{g}{m^2}\right) \quad (3)$$

Where (C_0) is denotes the concentration of the gas at the stack.

Wind power

In the lower part of the earth's boundary layer (the surface layer), the wind speed increases with height and exhibits a strong gradient near the ground. Thus, to describe the wind speed at the top of the stack, it's often calculated by a simple power law, by following equation (Anad *et al.,* 2022):

Fig. 2: Dataset sources, (a) 110-WS-25 standard weather station, (b) PS7400 system.

$$Uz = U_r\left(\frac{z}{zr}\right)^{\alpha} \quad (4)$$

Where (Uz) is Wind speed at height z ($m.s^{-1}$), (Ur) is Wind speed at reference height ($m.s^{-1}$), (zr) is Reference height at which wind speed is measured, (α) is Exponent reflecting surface roughness and atmospheric stability, with a value of 1/7 for neutral conditions over non-rough surfaces, rising to 0.25 in urban environments. A value of 1/7 was used in the study for a stack height of 60 meters (Liu *et al.,* 2024).

Atmospheric stability

The vertical response of air parcels, influenced by gradients in solar radiation and wind speed (Anad *et al.,* 2022), affects vertical motion and turbulence within the boundary layer, impacting aerosol and water vapor dispersion Stable conditions, characterized by low wind speeds and limited vertical mixing, lead to pollutant accumulation at the surface and deteriorated air quality. Conversely, unstable conditions, typically associated with sunny weather, promote extensive vertical mixing due to elevated temperatures and prolonged daylight, enhancing pollutant dispersion (Mahmood *et al.,* 2023). Atmospheric stability is assessed using the Pasquill classification system, which categorizes conditions into six distinct classes: very unstable (A), unstable (B), slightly unstable (C), neutral (D), slightly stable (E), and very stable (F). This classification takes into account various factors, including cloud cover, wind speed, and solar radiation. The Pasquill-Gifford (PG) chart was utilized to analyze meteorological data, specifically daily averages of solar radiation and wind speed, facilitating the evaluation of stability within the study area (Edokpa *et al.,* 2017), see Table 1.

Dispersion coefficients

In Gaussian plume models, the dispersion coefficients (σz and σy) are critical for estimating pollutant concentrations downwind of an emission source. These coefficients describe the dispersion of the plume in the horizontal σy and vertical σz directions. Specifically, σy represents the horizontal dispersion while σz represents the vertical dispersion. Both coefficients are standard deviations characterizing the spatial distribution of the plume. Their determination is based on stability class curves as shown in Fig. 3. By projecting the horizontal downwind distance onto these curves, σy and σz are calculated according to the atmospheric stability (Ogbozige, 2023).

Table 1: Pasquill-Gifford (PG) day time classification scheme

Wind Speed (at 10 m) (m/s)	Day time solar insolation			Radiation overcast
	Strong > 600 (W.m^{-2})	Moderate 300 – 600 (W.m^{-2})	Slight < 300 (W.m^{-2})	
<2	A	A - B	B	C
2 - 3	A - B	B	C	C
3 - 5	B	B - C	C	C
5 - 6	C	C - D	D	D
> 6	C	D	D	D

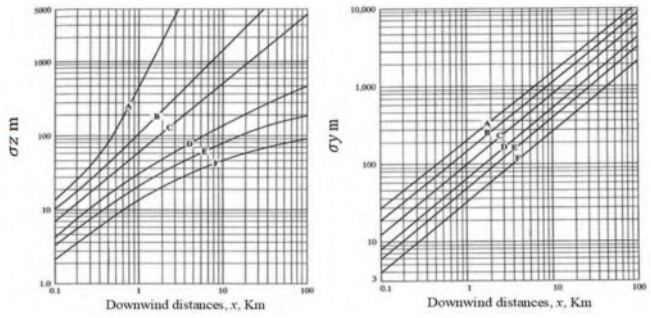

Fig. 3: Dispersion coefficient curve for σz and σy.

Modified Gaussian

In the study, surface-level pollutant concentrations were estimated using a modified Gaussian equation. Equation is based on the stipulation that modifications to the conventional Gaussian model were made for accurate prediction of ground-level concentration and evaluation of impact on human health and vegetation, as outlined in Equation (Brusca, 2016):

$$C\ (x.0.0) = \frac{Q}{2\pi\ U\ \sigma y \sigma z} \quad (5)$$

Where (Q) is represents the emission rate of each pollutant, (U) is wind speed at the top of a stack, ($\sigma y, \sigma z$ sigma-y and sigma-z) is the horizontal and vertical dispersion coefficients.

RESULTS AND DISSECTIONS

Daily variations in weather conditions

Climatic data collected at the Burjesia meteorological station included measurements of relative humidity, wind direction and speed, air temperature and solar radiation (Fig. 4). During the wet conditions, average solar radiation ranged from 150 to 200 W.m^{-2}, with significant decreases to 23 to 37 W.m^{-2} on certain days from December to March. Air temperatures varied between 15 and 23 °C, with maximum values of 32 °C in October and 37 °C in May. Wind speeds averaged between 2.5 and 3.5 m.s^{-1}, with a minimum of 1.5 m.s^{-1} recorded in October and a maximum of about 4.8 m.s^{-1} in February, March, April and May. Relative humidity varied between 50% and 70%, with significant decreases to around 23% in early October and late May. So, the increase in relative humidity at Basrah during the wet season (October to May) is due to various meteorological and environmental factors as follows:

1. Close to the Arabian Gulf and Shatt al-Arab River, which allow the penetration of humid marine air masses especially during cooler months.
2. Reduced Evaporation: During autumn, winter, and early spring, as a result of cooler temperatures and this period is characterized by occasional rainfall and increased cloud cover that helps in increasing the atmospheric moisture. So, less water evaporation and more precipitation and water remain in the atmosphere for longer periods of time.

Daily variations on the pollutants data (CO, SO_2, NO, and PM)

Continuous emissions monitoring systems (PS7400 Flue Gaseous System), equipped with sensors positioned within the stack of the Rumaila Combined Cycle Power Plant (RCCPP), recorded average daily concentrations of pollutants CO, SO2, NO, and PM in mg.m^{-3} throughout the wet conditions of 2023/2024. Daily measurements, illustrated in Fig. 5, indicated average CO concentrations ranging from 75 to 80 mg.m^{-3}, with a notable decrease to 101.89 mg.m^{-3} in May, because by May: temperatures' daily mean values oscillate between 23°C and 37°C, while levels of humidity drop from 73% in the initial days to 15% by the end. This necessitates more air conditioning, which is a key driver of increased electricity demand. Because Basrah depends fully on the national grid for uninterrupted power, the Rumaila Power Plant and other regional plants have to burn more natural gas in turbines: this is needed to meet the higher demands, especially in now-coming summertime, when it gets hotter and the cooling demand increases further. SO_2 concentrations varied between 18 and 35 mg.m^{-3}, also with a notable decrease to 0.65 mg.m^{-3} in end of April and beginning of May, because the purity of natural gas used is not of high quality in that period of the season. while NO levels ranged from 7 to 7.5 mg.m^{-3}, and PM concentrations fluctuated between 6 and 7.5 mg.m^{-3}.

Calculating the concentrations of gaseous CO, SO_2, NO, and PM volumetric flow rate

Fig. 6 depicts the volumetric emission rates measured under standard conditions (20°C and 1 atm) by Eq. 1, ranging from 500 to 650 kg.h^{-1}, in order to the condition inside the stack not standard we used Eq. 2. Corrections for variations in moisture content, pressure in atm unit, and temperature in kelvin unit inside the stack were applied for conversion of emission rates from kg.h^{-1} to g.s^{-1}, yielding emission rates of 0.2 to 0.7 g.s^{-1}. The conversion of emission rates from kg.h^{-1} to g.s^{-1} is imperative for several reasons. Emission measurements tend to be more precise when expressed in smaller units, such as g.s^{-1}, which is particularly significant in environmental applications that demand a high level of detail. Furthermore, many environmental standards and regulations specify emission limits in g.s^{-1}, making this conversion essential for

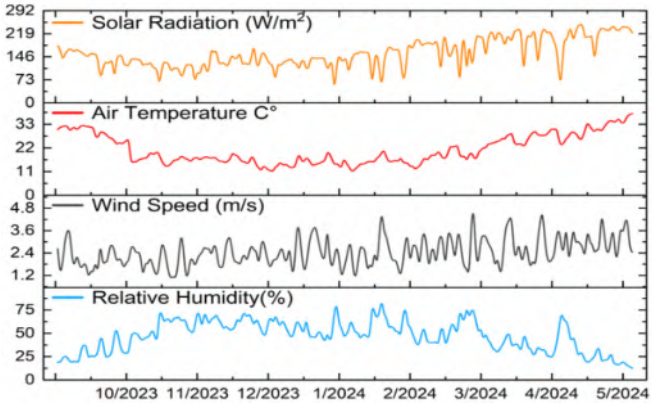

Fig. 4: Daily atmospheric elements, (a) solar radiation, (b) air temperature, (c) wind speed, (d) relative humidity, within wet conditions.

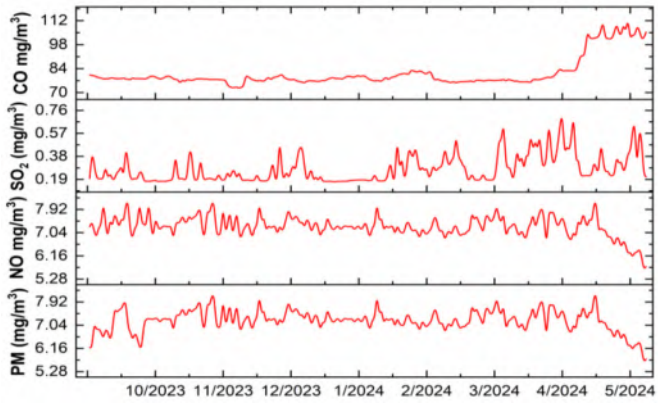

Fig. 5: Daily average concentration of pollutants CO, SO2, NO, and PM within wet conditions.

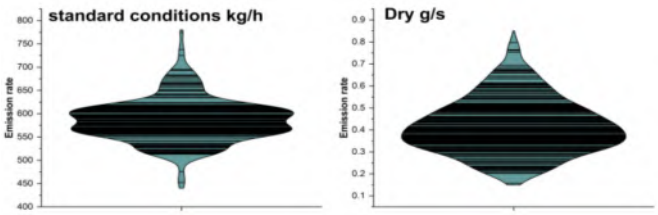

Fig. 6: Volumetric flow rate corrected based on Eq. 2.

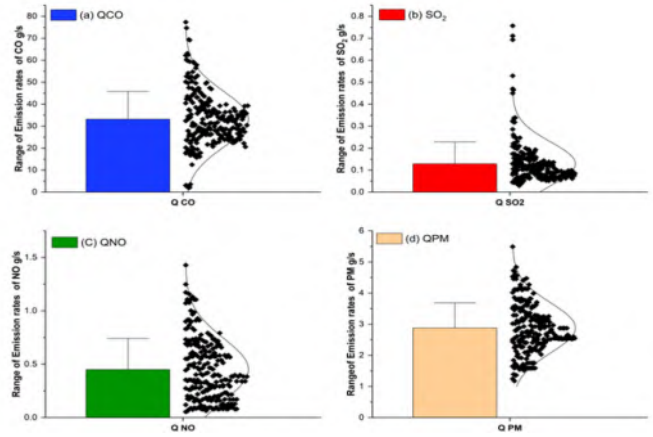

Fig. 7: CO, SO_2, NO, and PM emission rates as determined by Eq. 3.

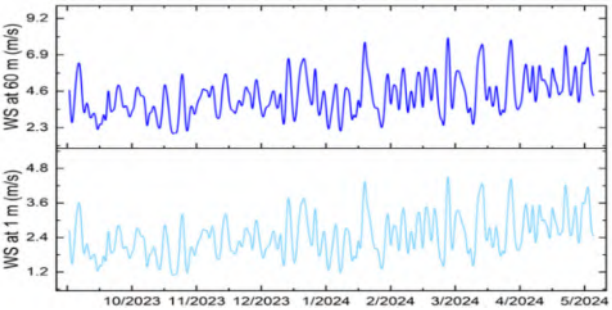

Fig. 8: wind speed at stack height.

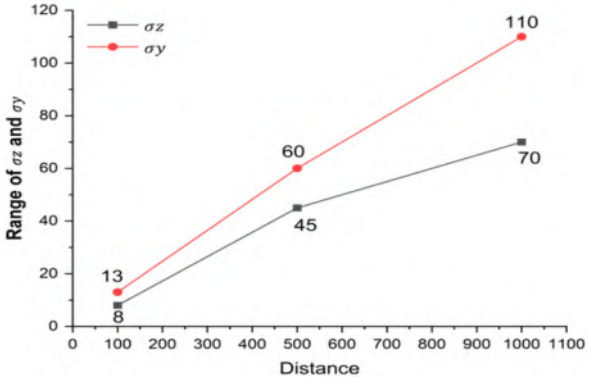

Fig. 9: σz and σy for three distances (100, 500, 1000 m).

compliance evaluations. Moreover, analyzing the initial dispersion of the emission plume is crucial for understanding pollutant behavior from point sources, such as stacks, and is vital for accurately assessing concentrations of air pollutants.

Pollutant emission rates: CO, SO_2, NO, and PM

The estimation of emission rates of carbon monoxide (CO), sulfur dioxide (SO2), nitrogen monoxides (NO), and particulate matter (PM) was made through Eq. 3 which included the use of pollutant concentrations in a unit $mg.m^{-3}$ with the dry volumetric emission rate. This critical adjustment is to have accurate modeling of pollutant dispersion. The emission rates were determined as: CO: 12 – 50 $g.s^{-1}$ SO_2: 0.02 – 0.1 $g.s^{-1}$ NO: 0.06 – 0.7 $g.s^{-1}$ PM: 0.02 $g.s^{-1}$, as shown in Fig. 7. Among these pollutants, CO emissions are elevated because of methane, the primary component of natural gas, and incomplete combustion due to either insufficient oxygen or low combustion temperatures. Inadequate ventilation with combustion systems further enhances levels of CO.

Wind speed at stack nozzle

Determining wind speed at the stack height of 60 meters is crucial for assessing pollutant concentrations. This measurement employs the exponential engineering wind law, as described in Eq. (4). This approach is particularly applicable to the RCCPP, situated in a flat desert region characterized by minimal surface roughness in the Rumaila Desert area of Al-Zubair District, Basrah Governorate. Analysis reveals a significant difference between wind speeds at 1 meter above ground and at the stack outlet. Data indicate that peak wind gusts were recorded at the end of the wet conditions, reaching approximately 4.8 $m.s^{-1}$. This increase in wind

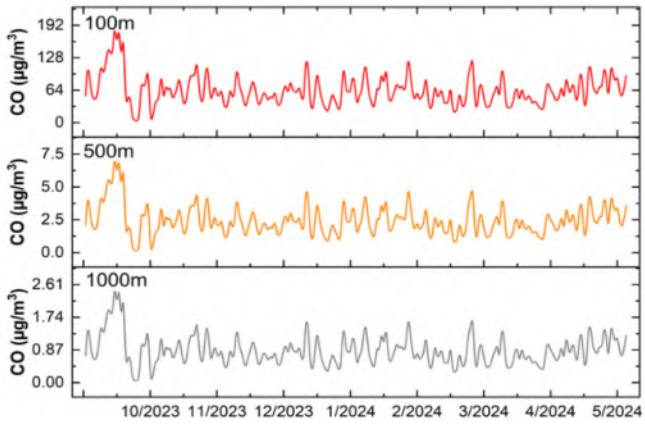

Fig. 10: CO concentration predictions for each day at distances 100, 500 and 1000 m within wet conditions.

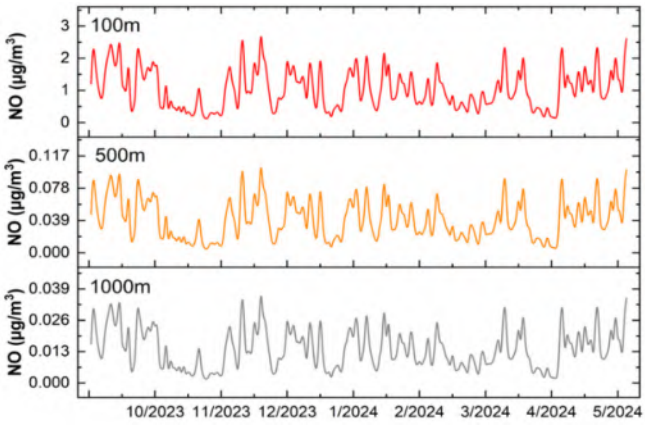

Fig. 12: NO concentration predictions for each day at distances 100, 500 and 1000 m within wet conditions.

speed correlates with rising temperatures, extended daylight hours, and decreasing humidity beginning in late February. These climatic factors collectively contribute to the observed gradual increase in wind speed during this period, as illustrated in Fig. 8.

Dispersion coefficients (σz and σy)

In this study, the atmospheric stability class was determined to be Class C (slightly unstable conditions), as indicated by Table 1, based on daily wind speed and solar radiation data. Using the stability class C curves from Fig. 3, we performed interpolation to calculate the vertical and lateral dispersion coefficients (σz and σy) at three specific distances: 100 meters, 500 meters, and 1000 meters from the RCCPP. The calculated dispersion coefficients are detailed in Fig. 9, which demonstrates that both (σz and σy) increase with increasing distance from the RCCPP. This trend reflects the dispersion characteristics of the atmospheric pollutants as they travel away from the emission source.

Application of simplified Gaussian equation

During the wet conditions of October 2023 to May 2024, concentrations of pollutants (CO, SO_2, NO, PM) were estimated at distances of 100 m, 500 m, and 1000 m from the RCCPP stacks. Using Eq. (5) alongside the dispersion coefficients (σz and σy) from Fig. 9 and the emission rates for each pollutant, we calculated

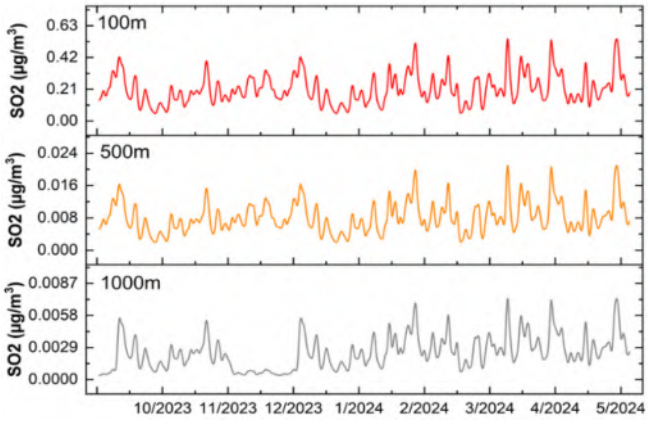

Fig. 11: SO_2 concentration predictions for each day at distances 100, 500 and 1000 m within wet conditions.

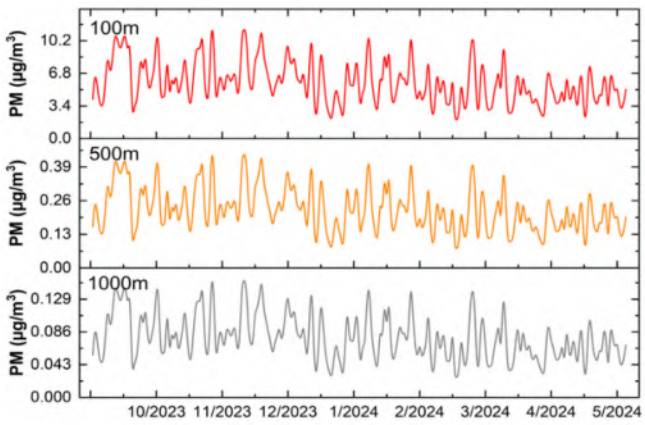

Fig. 13: PM concentration predictions for each day at distances 100, 500, and 1000 m within wet conditions.

the pollutant concentrations. To account for emissions from all five stacks at the RCCPP, the calculated concentrations were multiplied by a factor of 5 and converted unit of pollutants in $\mu g.m^{-3}$ in order to facilitate comparison with national determinants. The results, depicting daily concentrations for each pollutant at the specified distances, are shown in Figures 11, 12, 13, and 14. Generally, concentrations were highest at 100 m, decreased at 500 m, and were lowest at 1000 m. Notably, CO concentrations peaked at 185 $\mu g.m^{-3}$ at an altitude of 100 meters in October because during this period people are constantly consuming air conditioning devices, which requires high production from the RCCPP to meet people's needs. Despite this peak, most of the CO concentrations remained below the national ambient air quality standard of 960 $\mu g.m^{-3}$, as shown in Fig. 10.

Sulfur dioxide concentrations were assessed at distances of 100 m, 500 m, and 1000 m from the RCCPP using Eq. (5). The maximum recorded concentrations were 0.5 $\mu g.m^{-3}$, 0.05 $\mu g.m^{-3}$, and 0.01 $\mu g.m^{-3}$, respectively. These values are significantly below the national ambient air quality standard of 150 $\mu g.m^{-3}$ for a 24-hour period, indicating that SO_2 levels in the vicinity of the RCCPP with acceptable regulatory limits for air quality, as shown in Fig. 11.

Nitrogen monoxides (NO) concentrations during the wet conditions were estimated using a simplified Gaussian dispersion

model at distances of 100 m, 500 m, and 1000 m from the RCCPP. The highest recorded concentrations were 2.6 $\mu g.m^{-3}$ at 100 m, decreasing to 0.07 $\mu g.m^{-3}$ at 500 m and 0.03 $\mu g.m^{-3}$ at 1000 m. These values are significantly below the regulatory limit of 200 $\mu g.m^{-3}$, as illustrated in Fig. 12, indicating that NO concentrations near the power plant comply with acceptable air quality standards, as shown in Fig. 12.

Wet conditions average PM concentrations was estimated at distances of 100 m, 500 m and 1000 m from the power plant. The highest recorded concentrations were 11 $\mu g.m^{-3}$, 0.4 $\mu g.m^{-3}$, and 0.15 $\mu g.m^{-3}$, respectively. These concentrations are well below the national air quality standards for PM_{10} and $PM_{2.5}$, both by mathematical averages and in practice. The national air quality standards for PM_{10} and $PM_{2.5}$ are 150 $\mu g.m^{-3}$ and 35 $\mu g.m^{-3}$, as shown in Fig. 13.

CONCLUSIONS

The Rumaila Combined Cycle Power Plant, operational since 2018, combusts natural gas for base load operation. It processes approximately 4,500 cubic meters per second and produces 150–230 MWs of electricity per day. Emissions are released from five 60 m stacks. The current study, the first to characterize pollutant levels originating from this plant, is restricted to the regular emissions of combustion processes for natural gas. It is not appropriate for detailed conditions of pollutant dispersion at this plant stack. Our evaluation, sampling pollutant levels at different distances from the stacks, confirmed that the emissions are continually below National Ambient Air Quality Standards at ground level. This indicates little environmental impact and is due to the efficient plant design and stack height, plus location in a remote desert area where surface winds blow toward the population center an average of only 15 percent of the time and disperse pollutants well before reaching significant levels. If this low impact is to be retained, then we recommend implementing a continuous monitoring program to determine the influence of meteorological conditions on dispersion.

ACKNOWLEDGEMENT

The authors would like to thank the Ministry of Electricity, and Kar company for their access to the data of pollutants monitored through their devices.

Conflict of Interests: The authors of this paper affirm that they have no competing interests.

Funding: For the study they submitted, the authors received no support from any organizations.

Data availability: Permission to use the data was obtained from the Iraqi Ministry of Electricity and from the gas analyzer (CO, SO_2, NO, PM) belonging to Kar Investment Company. The meteorological data (SR, AT, WS, RH) were obtained from Al-Burjesia Agricultural Meteorology Station (related to Al-Zubair district, the same district as power plant RCCPP). All data are for October 2023 – May 2024

***Author contribution*: M. S. Nasser:** Data checked, processed, analyzed, and presented, Investigation, Writing-original draft; **Jinal S. AL-Hassany and Monim H. AL-Jiboori:** Supervision, editing, presented, Investigation and writing review.

Disclaimer: The contents, opinions and views expressed in the research article published in the Journal of Agrometeorology are the views of the authors and do not necessarily reflect the views of the organizations they belong to.

Publisher's Note: The periodical remains neutral with regard to jurisdictional claims in published maps and institutional affiliations.

REFERENCES

Abdel-Razzaq, F. A. W., Yaseen, S. K. and Dhaigham, A. A. R. (2023). Design and construction of anair pollution detection system using a laser beam and absorption spectroscopy. *Baghdad Sci. J.,* 20(3): 0825-0825. https://dx.doi.org/10.21123/bsj.2022.7650

Al-Muhyi, A. H. A. and Aleedani, F. Y. K. (2022). Impacts of global climate change on temperature and precipitation in basra city, iraq. *Basrah J. Sci.,* 40(1): 215-230. https://doi.org/10.29072/basjs.20220113

Anad, A. M., Hassoon, A. F. and Al-Jiboori, M. H. (2022). Assessment of air pollution around Durra refinery (Baghdad) from emission NO2 gas at April Month. *Baghdad Sci. J.,* 19(3): 0515-0515. http://dx.doi.org/10.21123/bsj.2022.19.3.0515

Anand, M. and Pal, S. (2023). Exploring atmospheric boundary layer depth variability in frontal environments over an arid region. *Boundary-Layer Meteorol.,* 186(2): 251-285. https://doi.org/10.1007/s10546-022-00756-z

Beychok, M. (1994). Fundamentals of stack gas dispersion (3rd ed). *Atmos. Environ.,* 29 (22): 193. https://doi.org/10.1016/1352-2310(95)90214-7

Brusca, S., Famoso, F., Lanzafame, R., Mauro, S., Garrano, A. M. C. and Monforte, P. (2016). Theoretical and experimental study of Gaussian Plume model in small scale system. *Energy Procedia*, 101: 58-65. https://doi.org/10.1016/j.egypro.2016.11.008

Edokpa, D. O. and Nwagbara, M. O. (2017) . Atmospheric Stability Pattern over Port Harcourt, Nigeria. *J. Atmos. Poll.,* 5(1): 9-17. https://doi.org/10.12691/jap-5-1-2.

Ghosh, A., Chakraborty, P. S. and Balakannan, K. (2023). Environmental Impact Assessment from the Emission of Combined Natural Gas Cycle Power Plant. *Sustain. Agri, Food Environ. Res.,* 11. Doi: https://doi.org/10.7770/safer-V11N1-art2595

Jasim, I. M., Al-Kubaisi, A. A. and Al-Obaidy, A. M. J. (2018). Test the Efficiency of some Plants in the Tolerant of Air Pollution within the City of Baghdad. Iraq. *Baghdad Sci. J.,* 15(1): 0009-0009. http://dx.doi.org/10.21123/bsj.2018.15.1.0009

Karmaker, A. K., Rahman, M. M., Hossain, M. A. and Ahmed,

M. R. (2020). Exploration and corrective measures of greenhouse gas emission from fossil fuel power stations for Bangladesh. *J. Cleaner Prod.,* 244: 118645. https://doi.org/10.1016/j.jclepro.2019.118645

Khadir, J. M., Hassoon, A. F. H. and Al-Knani, B. A. (2024). Influence of atmospheric stability conditions on wind energy density in Ali Al-Gharbi region of Iraq. *J. Agrometeorol.,* 26(3): 279-289. https://doi.org/10.54386/jam.v26i3.2589

Liu, H., Chen, G., Hua, Z., Zhang, J. and Wang, Q. (2024). Wind Shear Model Considering Atmospheric Stability to Improve Accuracy of Wind Resource Assessment. *Processes*, 12(5): 954. https://doi.org/10.3390/pr12050954

Mahmood, D. A., Naif, S. S., Al-Jiboori, M. H. and Al-Rbayee, T. (2023). Study the relationships among stability parameters in the atmospheric surface layer adjacent to oil refinery, Baghdad. *In AIP Conf. Proceed.*, 2775(1): http://dx.doi.org/10.1063/5.0164382

Ogbozige, F. J. (2023). Gaussian Plume Model Design of Effective Stack Hight For Control of Industrial Emissions. *Malawi J. Sci. Technol.,* 15(1): 95-104. https://www.ajol.info/index.php/mjst/article/view/256353

Talib, A. H. and Zainab, A. (2021). Measurement of some Air Pollutantsin Printing Units and Copy Centers Within Baghdad City. *Baghdad Sci. J.,* 18(1): 0687-0687. http://dx.doi.org/10.21123/bsj.2021.18.1(Suppl.).0000

Vandani, A. M. K., Joda, F. and Boozarjomehry, R. B. (2016). Exergic, economic and environmental impacts of natural gas and diesel in operation of combined cycle power plants. *Energy Conv. Manag.,* 109: 103-112. https://doi.org/10.1016/j.enconman.2015.11.048

Wang, M., Xiao, M., Bertozzi, B., Marie, G., Rörup, B., Schulze, B. and Donahue, N. M. (2022). Synergistic HNO3–H2SO4–NH3 upper tropospheric particle formation. *Nature*, 605(7910): 483-489. https://doi.org/10.1038/s41586-022-04605-4

Wang, Y., Ni, T., He, B. and Xu, J. (2024). Life cycle environmental impact assessment of natural gas distributed energy system. *Sci. Reports,* 14(1): 3292. https://doi.org/10.1038/s41598-024-53495-1

Wu, L., Huang, K., Ridoutt, B. G., Yu, Y. and Chen, Y. (2021). A planetary boundary-based environmental footprint family: From impacts to boundaries. *Sci. Total Environ.,* 785: 147383. Doi: https://doi.org/10.1016/j.scitotenv.2021.147383